Power Electronics and Drives
Volume 7(42), 2022 DOI: 10.2478/pead-2022-0004

Power Electronics and Drives

Performance Evaluation of BB-QZSI-Based DSTATCOMUnder Dynamic Load Condition

Research paper

Mrutyunjaya Mangaraj[1], Jogeswara Sabat[1*], Ajit Kumar Barisal[2], Anil Kumar Patra[3] and Ashok Kumar Chahattaray[4]

[1]*Department of Electrical & Electronics Engineering, Lendi Institute of Engineering & Technology, Vizianagaram, India-535005*
[2]*Department of Electrical Engineering, Odisha University of Technology and Research, Bhubaneswar, India-751029*
[3]*Department of Electrical & Electronics Engineering, Kalam Institute of Technology, Berhampur, India-761003*
[4]*Department of Electrical & Electronics Engineering, National Institute of Science and Technology, Berhampur, India-761008*

Received: January 21, 2022; Accepted: March 09, 2022

Abstract: This paper presents the shunt compensation performance of quasi-Z-source inverter (QZSI) and back to back connected QZSIs (BB-QZSI) to address the power quality (PQ) issues in the three-phase three-wire power utility network (PUN). Generally, these PQ issues are poor voltage regulation, low power factor (PF), source current distortion, unbalanced voltage, etc. The proposed BB-QZSI-based distribution static compensator (DSTATCOM) consists of two QZSIs with a common dc-link capacitor. Because the QZSI could achieve buck/boost conversion as well as DC to AC inversion in a single-stage and the back to back configuration decreases the system down time cost (if a fault occurs in one QZSI the other can continue the shunt compensation). Particularly, $icos\phi$ control algorithmcontrol algorithm is implemented to generate proper switching pulses for the switches of DSTATCOM. The effectiveness of the BB-QZSI is verified through simulation studies over QZSI using MATLAB/Simulink software satisfying the recommended grid code.

Keywords: *BB-QZSI • DSTATCOM • icosϕ control algorithm • PUN*

1. Introduction

Nowadays, different topologies of power electronics-based custom power devices are available due to the launch of active power filters to reduce the power quality (PQ) issues in three-phase power utility networks (PUN) (Bayu, 2020; Mangaraj and Sabat, 2021). In recent years, the integration of shunt compensators with low and medium voltage PUN has gained significant popularity (Bayu, 2020; Sabat et al., 2021). Clients ranging from domestic to industrial are demanding the utility companies to enhance the quality of power delivered. Power electronics devices integrated with unbalanced reactive loads generate PQ problems introducing source currents that are'distorted and unbalanced' (Mangarajand Sabat, 2021; Patel and Makwana, 2021). Generally, capacitor banks and passive filters are employed to enhance the PQ in PUN. But, some demerits have been observed inthese devices such as system parameters being dependent on performance, resonance with line reactance and compensation limit (Bayu, 2020).

The conventional two-level voltage source inverter (VSI) is frequently used as a common device to transfer the generated energy from the energy source to the PUN (Mangarajand Sabat, 2021; Ray et al., 2017). But an additional power stage conversion is required because VSI is a buck converter, which increases the cost and decreases the efficiency of the overall system (Reddivari and Jena, 2021). The above negative aspects of VSI decreases itsreliability and flexibility. To overcome the limitations of the VSI, an impedance source inverter (ZSI) is developed (Roomi, 2019). It performs both buck/boost functions (Liand Cheng, 2018; Roomi, 2019). The configuration of ZSI consists of an impedance network (X-shaped), which use two inductors and two capacitors. The advantages of ZSI are its ability to supply higher AC voltage compared to VSI and protectingthe inverter bridge from open and short circuits(Chauan et al., 2018; Liand Cheng, 2018;Roomi, 2019). But ZSI also hassome disadvantages such as

* *Email: jogesh.electrical@gmail.com*

more stress on the capacitors, low boost factor and discontinuous input current. To overcome the disadvantages of ZSI, a Quasi Z-source inverter (QZSI) is suggested because it can absorb constant power from the input side (Mohammadi et al., 2018). It consists of two capacitors, two inductors, a DC source and a diode (Bayhan et al., 2016). The operation of QZSI comprises of two states. During state-1(active state), it operates as a conventional VSI but during state-2 (shoot-through state), two switches of one leg of the inverter are switched ON simultaneously. Most significantly, shoot-through (state-2 operation) is allowed in the QZSI, whereby the upper and lower switches of each inverter leg can be switched on at the same time, which eliminates dead-time to reduce output waveform distortion (Bhavan et al., 2016;Battiston et al., 2016; Gu et al., 2018; Mohammadi et al., 2018).

In recent years, back to back connected configuration with common self-supported capacitors received more attention due to its ability to provide continuous input current and reduced component stress in the impedance network (Friedli et al., 2012; Mahatoet al., 2020; Tang et al., 2015; Zhou et al., 2016). Also, the back to back connected QZSIs (BB-QZSI) topology has attained the ability to mitigate the PQ issues as per the recommended standard grid code (Car et al., 2021). Hence, it is introduced as a new segment in low- and medium-voltage PUN.

A distribution static compensator (DSTATCOM) is a shunt compensator, which uses force commutated power electronics insulated gate bipolar transistors (IGBT) to improve PQ and control power flow. Also, it is a fast-acting device that regulates the voltage at the point of common coupling (PCC) by absorbing or providing reactive current (Mangaraj and Sabat, 2021and Sabat and Mangaraj, 2021). The $icos\phi$ control scheme permits a smooth transition from the steady-state operation into the unbalanced operation of a three-phase PUN while suppressing the PQ issues (Mangaraj et al., 2020; Mangaraj et al., 2020). The significant features of the control technique are listed as follows:

- Simple and error-free computation to extract the active and reactive parts of the fundamental load current (Mangaraj et al., 2020;Mangaraj and Sabat, 2021).
- Toughness, tracking and adaptive abilities are the initial findings of this control algorithm (Mangaraj and Sabat, 2021).

Better source current shaping, switching stress reduction, dc-link voltage reduction, improvement in voltage regulation and three-phase balance voltage obtained at the PCC of PUN (Mangaraj et al., 2020).

The original contribution of the BB-QZSI-based DSTATCOM topology is as follows:

- To the best of the author's knowledge, the shunt compensation of the BB-QZSI under PQ issues using $icos\phi$ control algorithm has not been investigated before this research work.
- The connected total nonlinear load current is divided by QZSI-1 and QZSI-2. Hence, it reduces the failure percentage of IGBT. When one QZSI shuts down, the other can continue the operation. Hence, it decreases the energy lost and downtime cost and ultimately reliability is increased.
- The simulation results highlight the performance of shunt compensation and the results obtained from BB-QZSI are better as compared to QZSI.
- The significant contributions of BB-QZSI are identified andthey are reduced switching stress, balanced voltage at PCC, power factor (PF) correction, source current shaping, etc.

In this article, the circuit description with the operation of the BB- QZSI is presented in Section 2. The $icos\phi$ control technique is presented in Section 3 and applied to QZSI integrated DSTATCOM. Section 4 describes the simulation performance of the topologies by showing the effectiveness of the DSTATCOM. Section 5concludes the paper by pointing to the salient features and the performance of BB-QZSI over QZSI.

2. PUN Operation And Design Of BB-QZSI-Based DSTATCOM

A dynamical three phase three wire PUN with BB-QZSI-based DSTATCOM, one non-linear load and three-phase balance sources which complete the utility network is depicted in Figure 1. PCC is a suitable point where the PUN, non-linear load and shunt compensator are connected together. Also, it is a convenient point to transfer the electric power between the load and PUN. In Figure 1, the three-phase supply, current sensitive three-phase non-linear load (diode bridge rectifier with resistor 'R' and inductor 'L') and BB-QZSI-based DSTACOM are connected at the PCC of PUN. The non-linear load draws three-phase load currents (i_{la}, i_{lb}, i_{lc}) from the three-phase balanced supply voltage (v_a, v_b, v_c). The PUN supplies the source currents (i_{sa}, i_{sb}, i_{sc}) to the connected load interfacing the distribution line impedance 'Z_s'. The BB-QZSI topology consists of two back to back connected QZSIs represented in Figure 1 as QZSI-1 and QZSI-2. A self-supported capacitor 'C' is connected to the input side of BBC-QZSI- based DSTATCOM

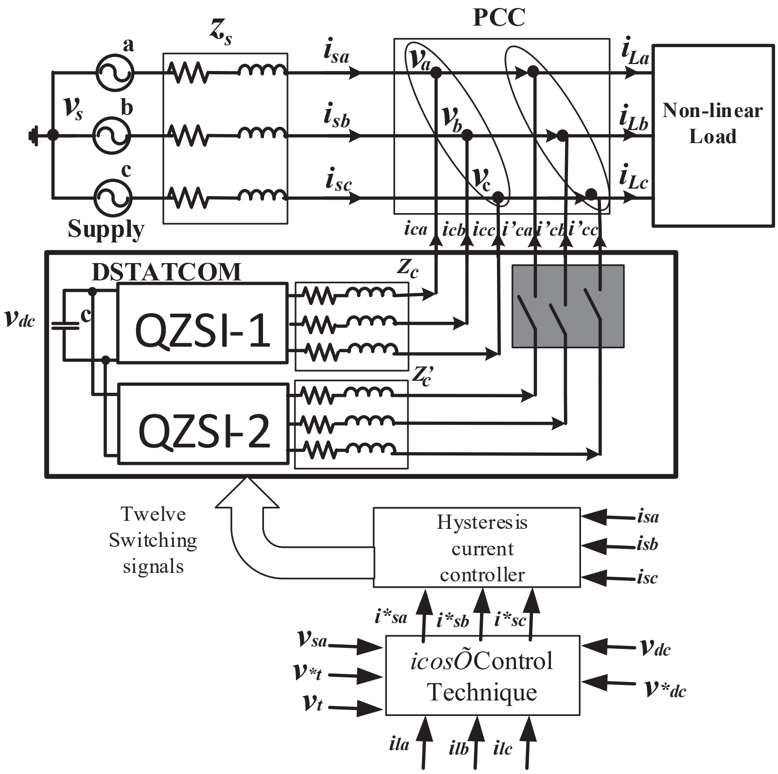

Fig. 1. Circuit diagram of the PUN and BB-QZSI-based DSTATCOM. BB-QZSI, back to back connected QZSIs; DSTATCOM, distribution static compensator; PCC, point of common coupling; PUN, power utility network; QZSI, Quasi Z-source inverter.

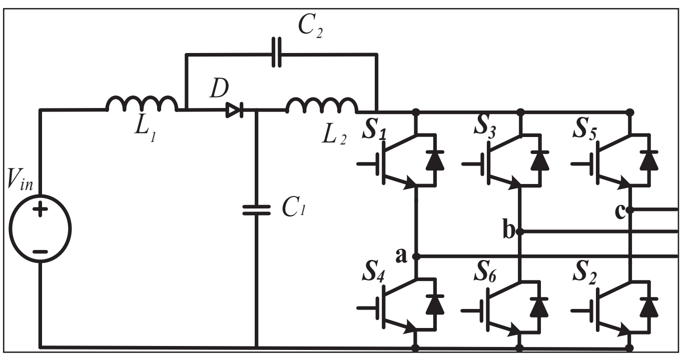

Fig. 2. Circuit configuration of QZSI. QZSI, Quasi Z-source inverter.

as shown in Figure 1. Both QZSI-1 and QZSI-2 are supplied from a common dc-link voltage (V_{dc}). The BBC-VSI-based DSTATCOM supplies the compensating currents (i_{ca}, i_{cb}, i_{cc}) from QZSI-1 and ($i'_{ca}, i'_{cb}, i'_{cc}$) from QZSI-2.

A single self-supported capacitor supports both QZSIs to reduce the PQ issues. Each QZSI is constructed having threelegs (two switches in each leg). Hence, a total of six switches are used. It attains 2^6 or 64 switching combinations during DSTATCOM operation. Figure 2 represents the QZSI configuration which consists of two capacitors, two inductors, a DC source and a diode. Generally, IGBTs are preferred for high voltage, high current and low switching frequency circuits. In IGBT, a transistor is shunted by a flyback diode to conduct current in the opposite direction because reverse current flow is required in bridge circuits. Also, when a load is disconnected, the inductive load current produces high voltage peaks which requires a suitable path otherwise it will destroy the switch.

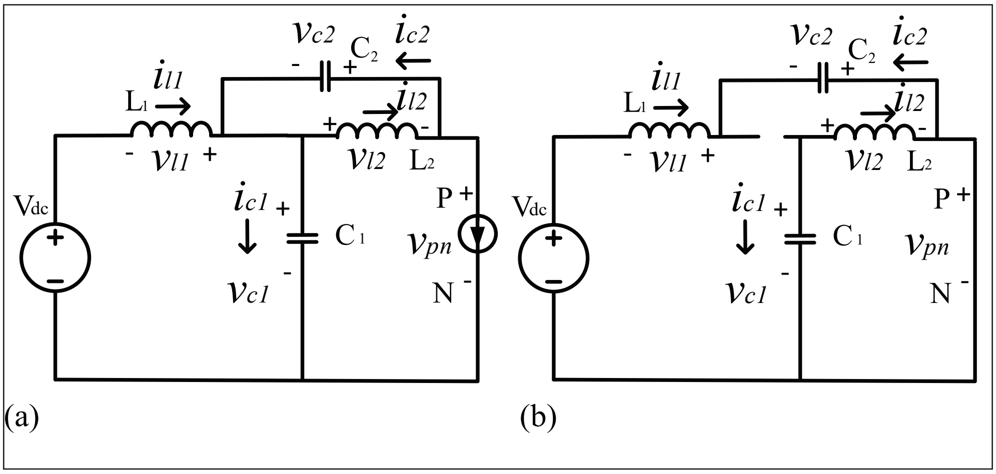

Fig. 3. QZSI circuit considers for analysis (a) Non-shoot through state and (b) Shoot through state. QZSI, Quasi Z-source inverter.

The QZSI configuration consists of two capacitors, two inductors, a DC source and a diode. The Z-network of the QZSI offers several advantages such as the ability to handle wide input voltage, constant DC from source and lower component ratings. Analysing the QZSI configuration during both non-shoot and shoot through states, different parameters are calculated. The shoot-through state and non-shoot through states of QZSI are depicted in Figure 3a and b, respectively.

Note that, T = switching period, T_0 = time period during shoot through state, T_1 = time period during non-shoot through state and

$$T = T_0 + T_1 \tag{1}$$

$$\text{and} \quad D = \frac{T_0}{T}, \text{ where } D = \text{ duty cycle} \tag{2}$$

Applying Kirchhoff's voltage and current laws in Figure 3a, we have

$$L_1 \frac{di_{l1}}{dt} = V_{dc} - V_{c1}, \tag{3}$$

$$L_2 \frac{di_{l2}}{dt} = -V_{c2}, \tag{4}$$

$$C_1 \frac{dV_{c1}}{dt} = i_{l1} - i_{PN} - i_{c1}, \tag{5}$$

$$C_2 \frac{dV_{c2}}{dt} = i_{l2} - i_{PN} - i_{c2}. \tag{6}$$

Similarly, applying Kirchhoff's voltage and current laws in Figure 3b, we get

$$L_1 \frac{di_{l1}}{dt} = V_{dc} + V_{c2}, \tag{7}$$

$$L_2 \frac{di_{l2}}{dt} = V_{c1}, \tag{8}$$

$$C_1\frac{dV_{c1}}{dt}=i_{l2}-i_{c1,} \tag{9}$$

$$C_2\frac{dV_{c2}}{dt}=-i_{l1}-i_{c2.} \tag{10}$$

The instantaneous voltage and current equations are given by

$$V_{c1}=\frac{1-D}{(1-2D)}V_{dc}, \tag{11}$$

$$V_{c2}=\frac{D}{(1-2D)}V_{dc,} \tag{12}$$

$$i_{l1}=\frac{D.i_{c2}+(1-D)i_{c1}+(1-D)i_{PN}}{1-2D}, \tag{13}$$

$$i_{l2}=\frac{D.i_{c1}+(1-D)i_{c2}+(1-D)i_{PN}}{1-2D}. \tag{14}$$

$\widetilde{V_{PN}}$ = Maximum dc-link voltage and the corresponding parameters are found by the following equations

$$\widetilde{V_{PN}}=V_{c1}+V_{c2,} \tag{15}$$

$$i_{l2}-i_{l1}=i_{c1}+i_{c2}, \tag{16}$$

$$P_{dc}=i_{dc}V_{dc,} \tag{17}$$

$$P_{c1}=i_{c1}V_{c1}\,, \tag{18}$$

$$P_{c2}=i_{c2}V_{c2.} \tag{19}$$

Gate signals for switches of QZSI are estimated by using the $\mathrm{i}\cos\phi$ control algorithm.

2.1. Design of parameters V_{dc}, C and L

The V_{dc} across the self-supported capacitor of BB-QZSI is taken as 1.6 times the peak of phase voltage (Battiston et al., 2016). Rating of the capacitor depends upon the variation of V_{dc}. The maximum energy exchanged by the BB-QZSI during the transient period is equal to the change in the capacitor's stored energy.

Note that the energy exchanged by the BB-QZSI during transient period = *nST* and the energy stored by the capacitor = $\frac{1}{2}CV^2$ (*n* = No. of cycles taken by the controller, *S* is the rating of the load in kVA and *T* is the system period).

$$nST=\frac{1}{2}CV^2 \tag{20}$$

$$\text{since } V^2=\left(\left(V_{dc\,ref}\right)^2-\left(V_{dc\,allowed}\right)^2\right), \tag{21}$$

where, $V_{dc\,ref}$ and $V_{dc\,allowed}$ are the reference dc voltage and maximum permissible dc voltage across capacitor during transient period, respectively.

Putting Eq. (21) in Eq. (20), we get

$$nST = \frac{1}{2}C\left(\left(V_{dc\,ref}\right)^2 - \left(V_{dc\,allowed}\right)^2\right)$$

$$\text{Or,}\quad \frac{1}{2}C\left(\left(V_{dc\,ref}\right)^2 - \left(V_{dc\,allowed}\right)^2\right) = nST \tag{22}$$

$$(\text{where } V_{dc\,allowed} = 0.8 \times V_{dc\,ref})$$

The magnitude of interfacing inductance *L* is calculated using the following equation

$$L = \frac{1.6V_m}{4h_x f_{max}} \tag{23}$$

(where, h_x = hysteresis band = 0.5 and f_{max} = Maximum switching frequency).

3. *icosϕ* Control Algorithm

The control structure of the *icosϕ* technique is presented in Figure 4. The proposed system circuit diagram of the PUN and BB-QZSI-based DSTATCOM is depicted in Figure 1. The control technique for the shunt compensator

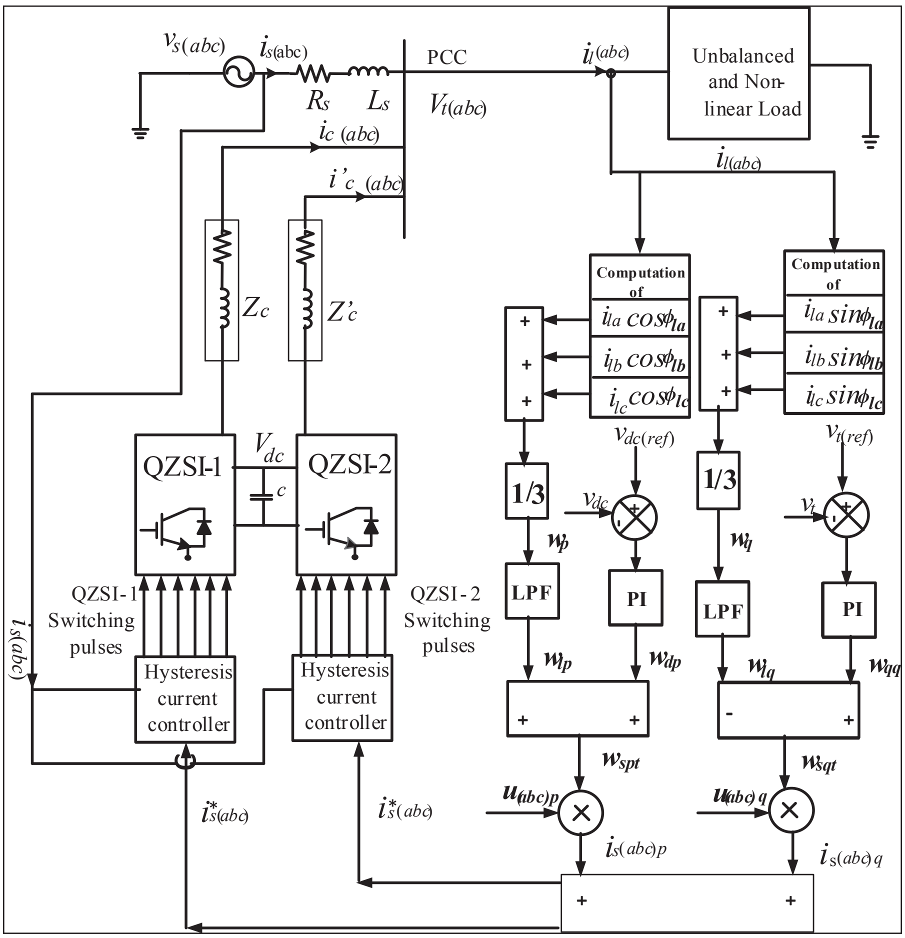

Fig. 4. System block diagram of icosϕ control technique. PF, power factor; QZSI, Quasi Z-source inverter.

generates the reference compensation currents to be supplied by the DSTATCOM at the PCC of PUN. The error-free minimum calculation steps choose the response time of the DSTATCOM. The control technique has the ability to mitigate the PQ issues like reduction in source current distortion, improvement in voltage regulation, balanced voltage at PCC and improvement in PF under both balanced and unbalanced loading conditions. In shunt compensation, the supply is supposed to supply the load current's active portion, here 'i' stands for the magnitude of the fundamental load current and '$icos\phi$' is the displacement PF of the connected load. Hence, it is named as $icos\phi$ control algorithm. The $icos\phi$ controller is used to generate the gate signals for switches of inverter and the selection of this technique is due to its fast and robust dynamic response to both steady-state and transient response (Mangaraj and Sabat, 2020a1, b; Singh and Bhuvaneswari, 2020).

Three steps are involvedin generating the gate signals for controlling the DSTATCOM:

- Fundamental quantities of the three-phase load current are computed using the Fourier block.
- The control technique is used to generate both active and reactive parts of the load current.
- The reference source current and actual source currentare given to the hysteresis current controller (HCC) to generate the switching pulses for the switches of the BB-QZSI.

The active component of fundamental load current can be computed using the below equation

$$\begin{bmatrix} i_{lap} \\ i_{lbp} \\ i_{lcp} \end{bmatrix} = \begin{bmatrix} Re\left(i_{la}\right) \\ Re\left(i_{lb}\right) \\ Re\left(i_{lc}\right) \end{bmatrix} = \begin{bmatrix} i_{la}cos\phi_{la} \\ i_{lb}cos\phi_{lb} \\ i_{lc}cos\phi_{lc} \end{bmatrix}, \tag{24}$$

where, i_{lxp} = amplitude of the active power component of load currents, $Re\left(i_{lx}\right)$ = Real part of the load currents, $i_{lx}cos\phi_{lx}$ = amplitude of load currents multiplies with the corresponding phase cosine of the phase angle and 'x' stands for phases a, b and c.

The magnitude of the 'w_p' (weighted active component of fundamental load currents average) can be expressed as

$$w_p = \left(\frac{i_{la}cos\phi_{la} + i_{lb}cos\phi_{lb} + i_{lc}cos\phi_{lc}}{3}\right). \tag{25}$$

In the same way, the reactive power component can be expressed as

$$\begin{bmatrix} i_{laq} \\ i_{lbq} \\ i_{lcq} \end{bmatrix} = \begin{bmatrix} Im\left(i_{la}\right) \\ Im\left(i_{lb}\right) \\ Im\left(i_{lc}\right) \end{bmatrix} = \begin{bmatrix} i_{la}sin\phi_{la} \\ i_{lb}sin\phi_{lb} \\ i_{lc}sin\phi_{lc} \end{bmatrix}. \tag{26}$$

The weighted average value of the reactive power component w_q is given as

$$w_q = \left(\frac{i_{la}sin\phi_{la} + i_{lb}sin\phi_{lb} + i_{lc}sin\phi_{lc}}{3}\right). \tag{27}$$

The proportional integral (PI) controller output is expressed as

$$w_{dp} = k_{pdp}v_{de} + k_{idp}\int v_{de}dt, \tag{28}$$

where, w_{dp} = total active components of the reference source currents, k_{pdp} =proportional controller, k_{idp} = integral controller and v_{de} = error in dc voltage.

The total active components of the reference source currentsare given as

$$w_{spt} = w_{dp} + w_{lp}. \tag{29}$$

In the same manner, the total reactive components can be computed from

$$w_{sqt} = w_{qq} - w_{lq}. \tag{30}$$

A 20 Hz cut-off frequency low-pass filter (LPF) is utilized for filtering of load current ripple.
The instantaneous value of the active source currents i_{sp}, can be computed from

$$\begin{bmatrix} i_{sap} \\ i_{sbp} \\ i_{scp} \end{bmatrix} = w_{spt} \begin{bmatrix} u_{ap} \\ u_{bp} \\ u_{cp} \end{bmatrix}. \tag{31}$$

The instantaneous value of the reactive source currents i_{sq} , can be computed from

$$\begin{bmatrix} i_{saq} \\ i_{sbq} \\ i_{scq} \end{bmatrix} = w_{sqt} \begin{bmatrix} u_{aq} \\ u_{bq} \\ u_{cq} \end{bmatrix}. \tag{32}$$

Finally, the reference source currents can be estimated from

$$\begin{bmatrix} i_{sa}^{*} \\ i_{sb}^{*} \\ i_{sc}^{*} \end{bmatrix} = \begin{bmatrix} i_{sap} \\ i_{sbp} \\ i_{scp} \end{bmatrix} + \begin{bmatrix} i_{saq} \\ i_{sbq} \\ i_{scq} \end{bmatrix}. \tag{33}$$

The reference source currents (i_{sa}^{*}, i_{sb}^{*} and i_{sc}^{*}) and the actual source currents (i_{sa}, i_{sb} and i_{sc}) of each phase are compared, and then the current error signals are supplied to HCC. It operates as, when $i_{sa} < i_{sa}^{*}$, switch 1 is ON and switch 4 is OFF, similarly when $i_{sa} > i_{sa}^{*}$, switch 1is OFF and switch 4 is ON.

4. Simulation Results

The proposed $i\cos\phi$ control strategy is first simulated by using MATLAB software. At the start, the PUN is verified by connecting a current sensitive non-linear load, and the compensator is not connected at PCC. At this time, the distortion in source current is identical to the load current. The simulation model of the proposed PUN with BB-QZSI-based DSTATCOM is presented in Figure 5.Simulation results of BB-QZSI and single QZSI supported DSTATCOM using Sim power toolbox is designed and their outputs are presented in the following subsection:

4.1. Simulation results of QZSI integrated DSTATCOM under both steady-state and dynamic states

As shown in Figure 1, the proposed system is designed using MATLAB/Simulink. It consists of a balanced three-phase supply, current sensitive three-phase non-linear load (diode bridge rectifier with resistor '*R*=10 *Ω' and inductor 'L*=20 mH') and QZSI-based DSTATCOM. Here, the fundamental frequency and reference dc-link voltage of QZSI are 50 Hz and 600 V, respectively. The different important parameters of the designed system are provided in Table 1.

The QZSI current tracking characteristics under balanced and unbalanced loading conditions are depicted in Figure 6. The duration from 0.55 s to 0.6 s and 0.7 s to 0.75 s shows the balanced loading condition but the duration from 0.6 s to 0.7 s is considered for unbalanced loading condition. The QZSI dc-link voltage v_{dc} (ref) is varied from 700 V to 770 V during the unbalanced condition. Figure 7a and b represents the **Fast Fourier Transform** FFT analysis of source current and sensitive load current, respectively. But the Figure 7c and d waveforms represent the phase displacement of supply voltage and current before and after compensation, respectively. After compensation, the source current's total harmonic distortion (THD) is reduced to 4.66% and animprovement in PF 0.971 is found.

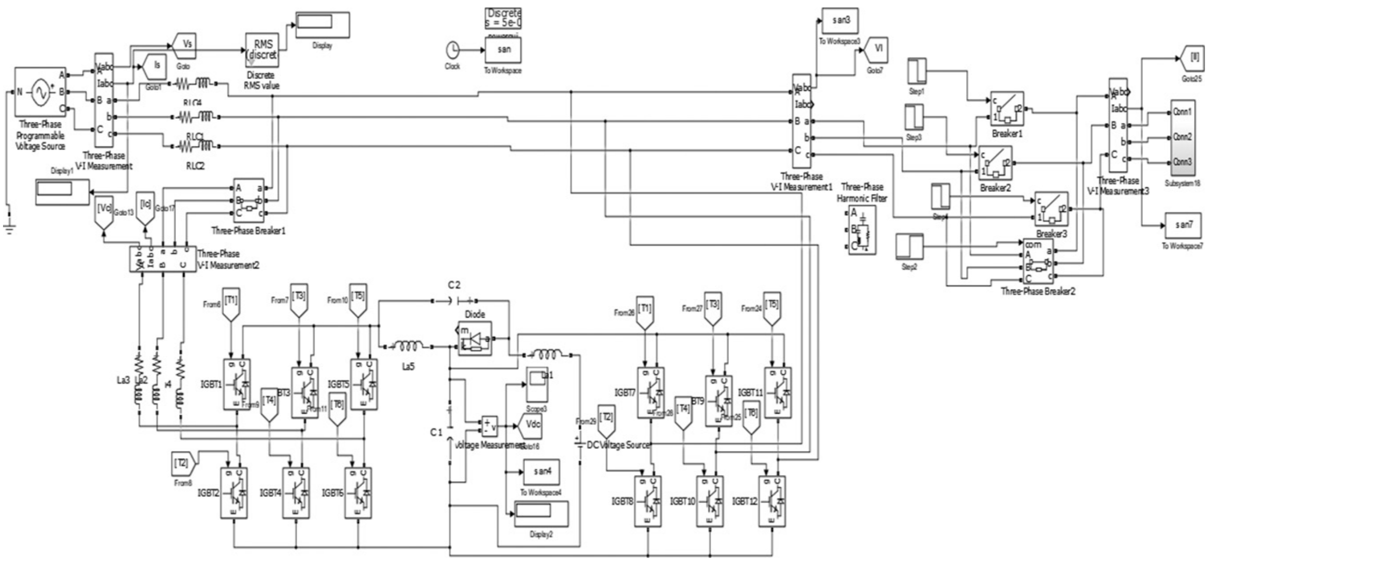

Fig. 5. Simulation model of the proposed PUN with BB-QZSI-based DSTATCOM. BB-QZSI, back to back connected QZSIs. DSTATCOM, distribution static compensator; PUN, power utility network; QZSI, Quasi Z-source inverter.

Table 1. Different parameters of the simulation study

Symbol	Detail	Magnitude
v_{dc}	dc-link voltage	600 V
C_{dc}	Capacitor	2,000 μF
k_{pdp}	Proportional controller gain	0.01
k_{idp}	Integral controller gain	0.05
R_c	Compensator resistance	0.25 Ω
L_c	Compensator inductance	1.5 mH
R_s	Source resistance	0.5 Ω
L_s	Source inductance	2 mH
v_s	Nominal supply voltage	230 V/phase
f_s	Nominal fundamental frequency	50 Hz
K_{pr}	Controller (AC proportional)	0.2
K_{ir}	Controller (AC integral)	1.1

4.2. Simulation results of BB-QZSI integrated DSTATCOM under both steady-state and dynamic state

The same parameters are used to build the proposed topology; instead of a single QZSI,dual QZSIs are connected back-to-back here. The dynamic and transient responses of BB-QZSI current tracking characteristics are depicted in Figure 8.

The duration of 0.55 s to 0.6 s and 0.7 s to 0.75 s shows the balanced loading condition but the duration from 0.6 s to 0.7 s is considered for unbalanced loading condition. Here, the reference dc-link voltage is varied from 600 V to 680 V during the unbalanced condition. After compensation, the source current THD% is reduced to 3.21% which is depicted in Figure 9a. The load current THD 29.75% is shown in Figure 9b. The phase displacements between the corresponding source voltage and current before and after compensation are depicted in Figure 9c and d, respectively.

Source current THD reduction must be taken into account to compare these two DSTATCOMs, this reduction in THD of PUN leads to a better performance of DSTATCOM and an increase in reliable and flexible operation

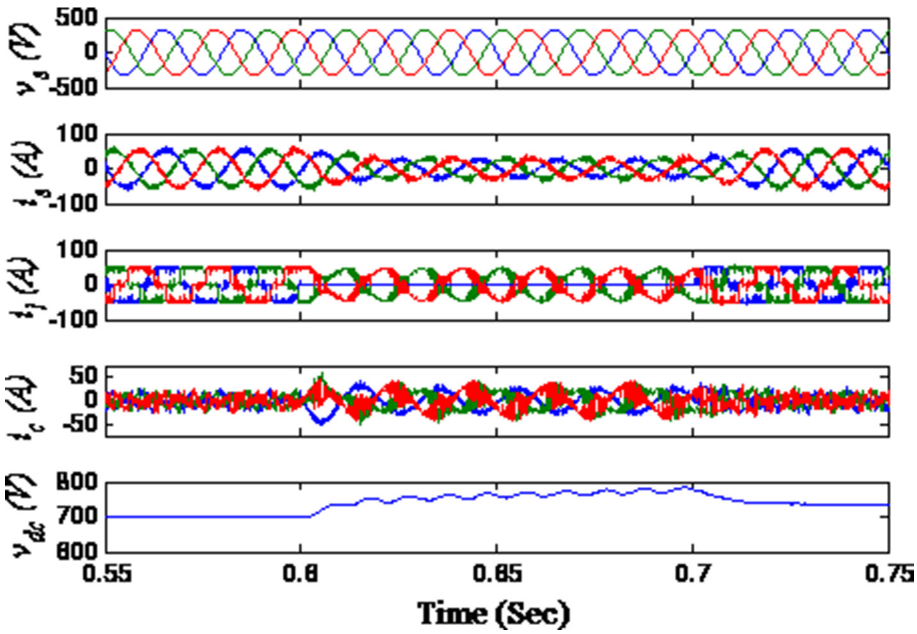

Fig. 6. Simulation waveform of three-phase supply voltage, three-phase supply current, three-phase load current, three-phase compensating current and QZSI dc-link voltage. QZSI, Quasi Z-source inverter.

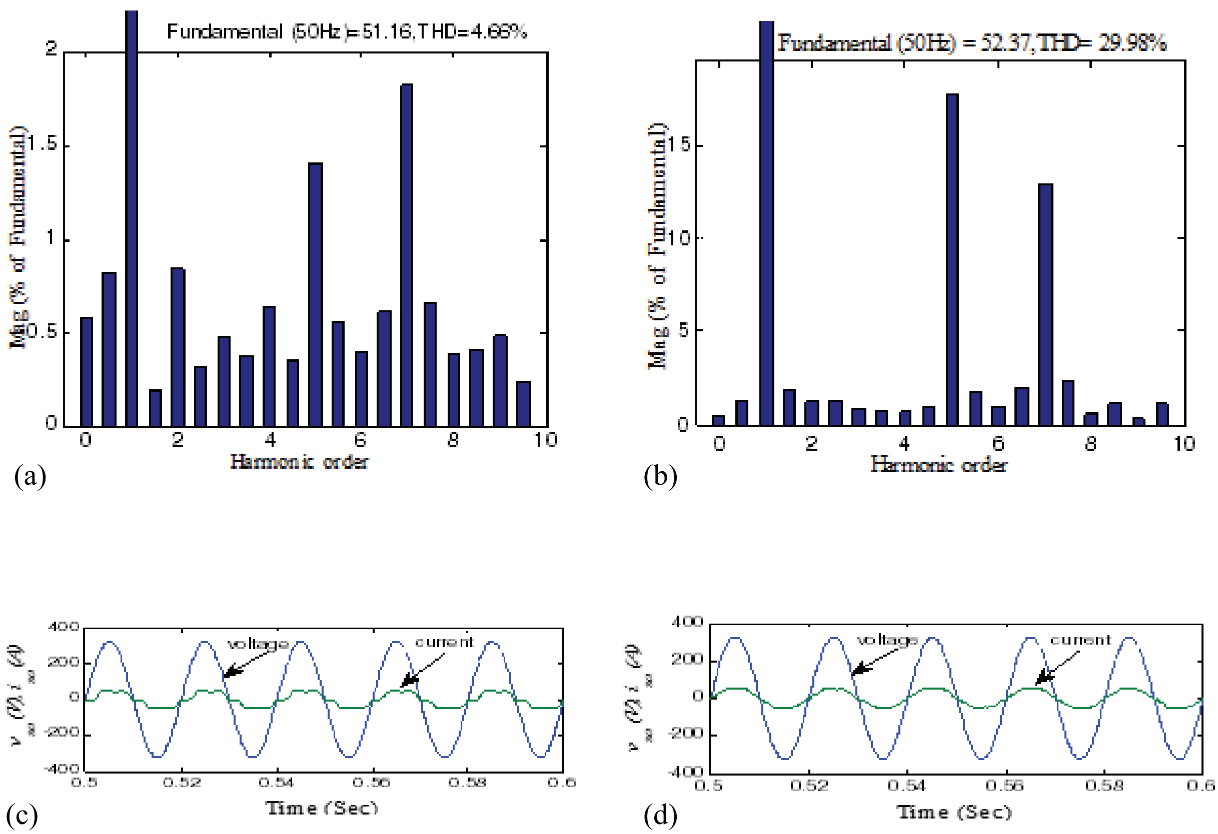

Fig. 7. Simulation results of QZSI, (a) spectrum analysis of source current after compensation i_s THD%, (b) spectrum analysis of load current after compensation i_l THD%, (c) before compensation phase displacement between the source voltage and source current and (d) after compensation phase displacement between the source voltage and source current.QZSI, Quasi Z-source inverter; THD, total harmonic distortion.

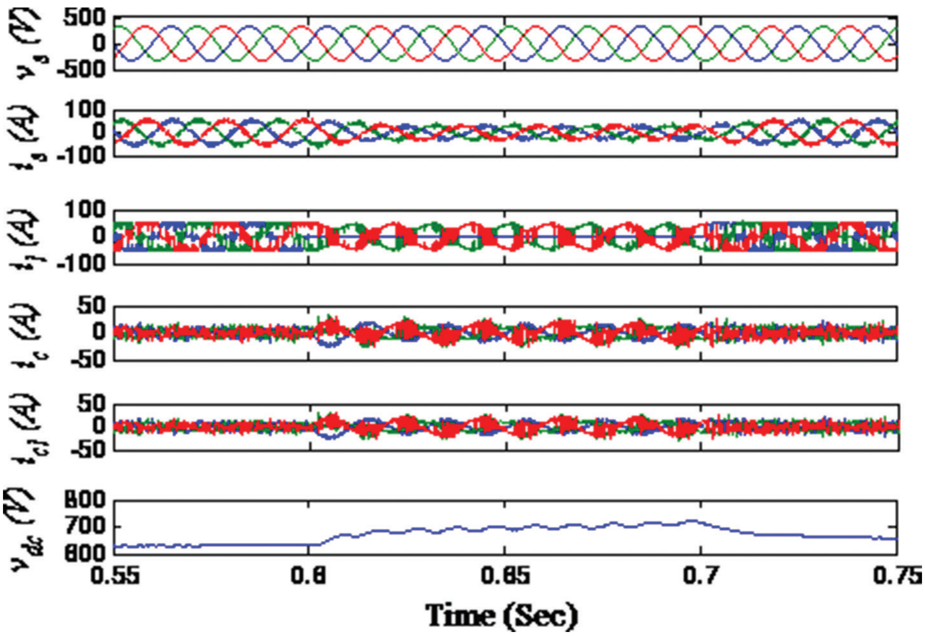

Fig. 8. Simulation waveform of three-phase supply voltage, three-phase supply current, three-phase load current, three-phase compensating current and QZSI dc-link voltage. QZSI, Quasi Z-source inverter.

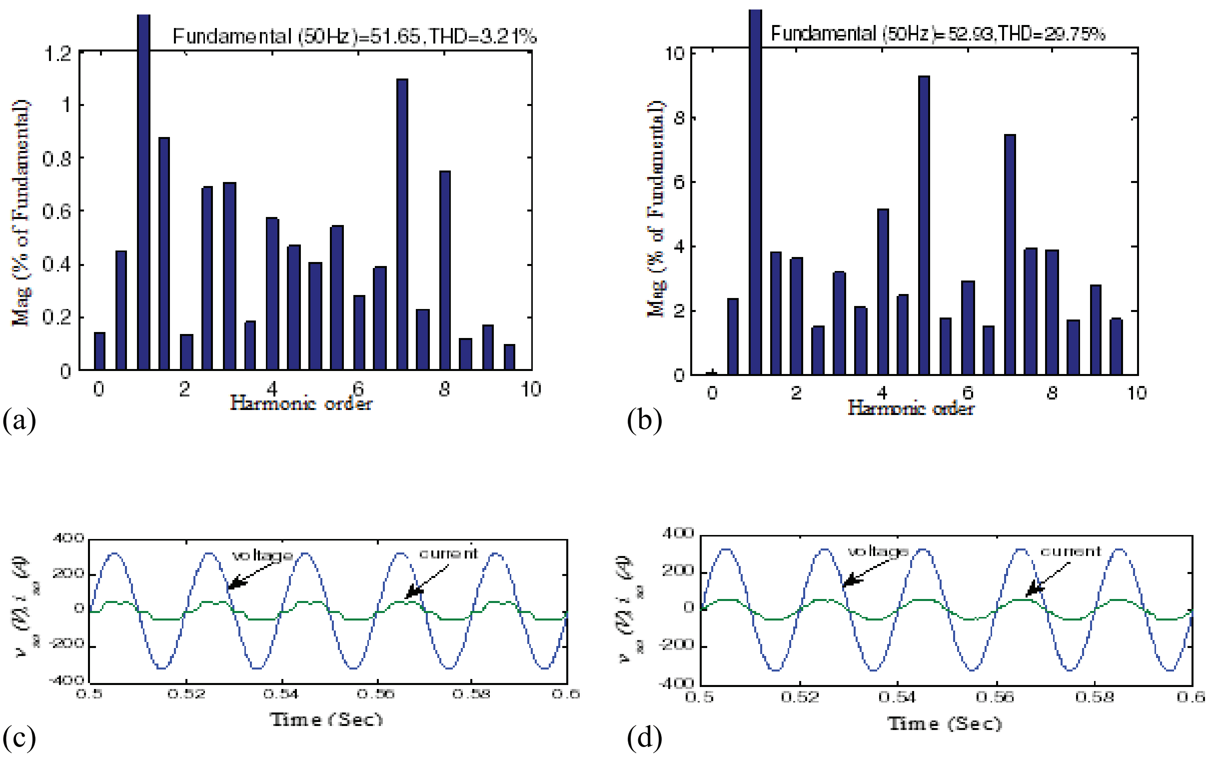

Fig. 9. Simulation results of BB-QZSI, (a) spectrum analysis of source current after compensation i_s THD%, (b) spectrum analysis of load current after compensation i_l THD%, (c) before compensation phase displacement between the source voltage and source current and (d) after compensation phase displacement between the source voltage and source current. BB-QZSI, back to back connected QZSIs. QZSI, Quasi Z-source inverter; THD, total harmonic distortion.

Table 2. Comparison between QZSI and BB-QZSI

DSTATCOM	Source current (i_s) (A), %THD	Load current (i_1) (A), %THD	PF	PCC voltage (V), %THD
QZSI	51.16, 4.66	52.37, 29.98	0.971	299.4, 1.23
BB-QZSI	51.65, 3.21	52.93, 29.75	0.983	299, 1.03

BB-QZSI, back to back connected QZSIs; DSTATCOM, distribution static compensator; PCC, point of common coupling; PF, power factor; QZSI, Quasi Z-source inverter; THD, total harmonic distortion.

Table 3. Comparison of BB-QZSI with other similar work

DSTATCOM	Source current THD%	Load current THD%	PF
BB-QZSI	3.21	29.75	0.9
Zhou et al. (2016)	3.8	27.9	0.8

BB-QZSI, back to back connected QZSIs; DSTATCOM, distribution static compensator; PF, power factor; QZSI, Quasi Z-source inverter; THD, total harmonic distortion.

with enhanced PQ. The performance parameters of single and BB- QZSI are shown in Table 2. The performance of BB-QZSI-based DSTATCOM under PQ issues with relevant similar work 'A High-Performance Microgrid With a Mechanical Sensor lessSynRG Operated Wind Energy Generating System' using back-to-back VSI configuration with a common dc-link is arranged in Table 3 (Zhou et al., 2016).

5. Conclusion

This work concludes that BB-QZSI with $icos\varnothing$ control strategy for PUN applications meets the demand of buck/boost single-stage conversion and reactive power compensation. It has the ability to get a better PQ and stability of PUN. Moreover, an inclusive evaluation between classic QZSI and BB-QZSI-based DSTATCOM has been projected to provide shunt compensation. Although both topologies-based DSTATCOM schemesdiffer in the THD reduction, still, it has been found that the BB-QZSI topology can efficiently eliminate source side harmonic reduction, minimize switching losses, voltage balancing at PCC, PF improvement and reasonable voltage regulation with system stability.Furthermore, it is shown that the BB-QZSI has good shunt compensation capability and can reduce the THD well below the limit of the grid code over QZSI.Based on the analysis made from theoretical propositions and simulated results, a typical BB-QZSI is finally suggested.

References

Battiston, A., Miliani, E. -H., Pierfederici, S. and Meibody-Tabar, F. (2016). Efficiency Improvement of a Quasi-Z-Source Inverter-Fed Permanent-Magnet Synchronous Machine-Based Electric Vehicle. *IEEE Transactions on Transportation Electrification*, 2(1), pp. 14–23, doi: 10.1109/TTE.2016.2519349.

Bayhan, S., Abu-Rub, H. and Balog, R. S. (2016). Model Predictive Control of Quasi-Z-Source Four-Leg Inverter. *IEEE Transactions on Industrial Electronics*, 63(7), pp. 4506–4516, doi: 10.1109/TIE.2016.2535981.

Bayu A. (2020). Power Quality Enhancement Using DSTATCOM in Industry Plants. *Power Electronics and Drives*, 5(40), pp. 157–175, doi:10.2478/pead-2020-0012.

Car, M., Lešić, V. and Vašak, M. (2021). Cascaded Control of Back-to-Back Converter DC Link Voltage Robust to Grid Parameters Variation. *IEEE Transactions on Industrial Electronics*, 68(3), pp. 1994–2004.

Chauhan, A. K., Raghuram, M. and Singh, S. K. (2018). Nonzero Discontinuous Inductor Current Mode in Certain Z-Source Converters.*IEEE Transactions on Power Electronics*, 33(4), pp. 2809–2814, doi: 10.1109/TPEL.2017.2754296.

Friedli, T., Kolar, J. W., Rodriguez, J. and Wheeler, P. W. (2012). Comparative Evaluation of Three-Phase

AC–AC Matrix Converter and Voltage DC-link Back-to-Back Converter Systems. *IEEE Transactions on Industrial Electronics*, 59(12), pp. 4487–4510.

Gu, Y., Chen, Y. and Zhang, B. (2018). Enhanced-Boost Quasi-Z-Source Inverter With an Active Switched Z-Network. *IEEE Transactions on Industrial Electronics*, 65(10), pp. 8372–8381, doi: 10.1109/TIE.2017.2786214.

Li, T. and Cheng, Q. (2018). A Comparative Study of Z-Source Inverter and Enhanced Topologies. *CES Transactions on Electrical Machines and Systems*, 2(3), pp. 284–288, doi: 10.30941/CESTEMS.2018.00035.

Mahato, B., Majumdar, S., Paul, S., Pal, P. K. and Jana, K. C. (2020). A New and Modular Back-to-Back Connected T-Type Inverter for Minimum Number of Power Devices, TSV, and Cost Factor. *IETE Technical Review*, pp. 1–8, doi: 10.1080/02564602.2020.1860838.

Mangaraj, M. and Sabat, J. (2020a). Two and Three-level Supported DSTATCOM Topologies for Compensation Analysis. *2020 International Conference on Computational Intelligence for Smart Power System and Sustainable Energy (CISPSSE)*, pp. 1–6, doi: 10.1109/CISPSSE49931.2020.9212219.

Mangaraj, M. and Sabat, J.(2020b). Comparative Analysis of Both Three & Fifth Level Based DSTATCOM Using IcosΘ Technique.*2020 International Conference on Computational Intelligence for Smart Power System and Sustainable Energy (CISPSSE)*, pp. 1–6, doi: 10.1109/CISPSSE49931.2020.9212272.

Mangaraj, M. and Sabat, J. (2021). Analysis and Control Design of Different Level VSI Based DSTATCOM. In: 2021 1st International Conference on Power Electronics and Energy (ICPEE), pp. 1–5, doi: 10.1109/ICPEE50452.2021.9358584.

Mangaraj, M. and Sabat, J. (2021). MVSI and AVSI-supported DSTATCOM for PQ Analysis. *IETE Journal of Research*, pp. 1–7, doi: 10.1080/03772063.2021.1920850.

Mangaraj, M., Naidu, V. D., Priyanka, K. and Sabat, J. (2020). Comparative Analysis between Inductor Coupled T Type Split and Self Supported Capacitor Based DSTATCOM. *2020 IEEE International Symposium on Sustainable Energy, Signal Processing and Cyber Security (iSSSC)*, 2020, pp. 1–5, doi: 10.1109/iSSSC50941.2020.9358812.

Mohammadi, M., Moghani, J. S. and Milimonfared, J. (2018). A Novel Dual Switching Frequency Modulation for Z-Source and Quasi-Z-Source Inverters. *IEEE Transactions on Industrial Electronics*, 65(6), pp. 5167–5176, doi: 10.1109/TIE.2017.2784346.

Patel, K. S. and Makwana, V. H. (2021). Modified Control Technique of DFIG for Power Quality Improvement. *IETE Journal of Education*, 62(1), pp. 44–54, doi: 10.1080/09747338.2021.1930591.

Ray, S., Gupta, N. and Gupta, R. A. (2017). A Comprehensive Review on Cascaded H-bridge Inverter-Based Large-Scale Grid-Connected Photovoltaic.*IETE Technical Review*, 34(5), pp.463–477,doi:10.1080/02564602.2016.1202792.

Reddivari, R. and Jena, D. (2021). A Correlatives Investigation of Impedance Source Network: A Comprehensive Review. *IETE Technical Review*, pp. 1–34, doi: 10.1080/02564602.2020.1870006.

Roomi, MM. (2019). An Overview of Carrier-based Modulation Methods for Z-Source Inverter. *Power Electronics and Drives*, 4(39), pp. 15–31. doi:10.2478/pead-2019-0007.

Sabat, J. and Mangaraj, M. (2021). GLMS Control Strategy Based DSTATCOM for PQ Enhancement, Modeling and Comparative Analysis. *Energy System*, pp. 1–20, doi: 10.1007/s12667-021-00489-x.

Singh, B. and Bhuvaneswari, G. (2020). A High-Performance Microgrid With a Mechanical SensorlessSynRG Operated Wind Energy Generating System. *IEEE Transactions on Industrial Informatics*, 16(12), pp. 7349–7359, doi: 10.1109/TII.2020.2976906.

Tang, C. Y., Chen, Y. F., Chen, Y. M. and Chang, Y. R. (2015).DC-link Voltage Control Strategy for Three-Phase Back-to-Back Active Power Conditioners. *IEEE Transactions on Industrial Electronics*, 62(10), pp. 6306–6316.

Zhou, D., Zhao, J. and Liu, Y. (2016). Independent Control Scheme for Nonredundant Two-Leg Fault-Tolerant Back-to-Back Converter-Fed Induction Motor Drives. *IEEE Transactions on Industrial Electronics*, 63(11), pp. 6790–6800.